

In search of the Stradivarius-like solutions  
in classical wave mechanics

Anna Lawless (10302989)

January 2014

With Maurese Gargan  
Supervised by Prof Mauro Ferreira

# Abstract

The aims of this project were to study solutions of the one dimensional wave equation in a material containing short-range scatterers, and to investigate the effect of these scatterers on the acoustic response of the material. The ultimate goal is to solve the inverse problem, i.e. to determine how the mass of a material should be spatially distributed in order to generate a specific wave response. The motivation comes from acoustic engineering and the construction of musical instruments, where the possibility of reproducing the response of Stradivarius instruments with ordinary pieces of wood is currently being investigated. By considering a highly simplified one dimensional case, this project aims to capture the essential physics of the problem. This is done using Green's function methods, and by demonstrating that the problem can essentially be reduced to that of solving the Schrödinger Equation of quantum mechanics for a "potential" composed of delta functions. It is found qualitatively that by varying the positions of the point scatterers, specific frequency responses can be generated. This is an important first step towards solving the inverse problem.



# Contents

<b>1</b>	<b>Introduction</b>	<b>4</b>
1.1	Motivation . . . . .	4
1.2	Simplifications and Assumptions . . . . .	5
<b>2</b>	<b>Theory and Methods</b>	<b>5</b>
2.1	The Wave Equation . . . . .	5
2.2	Green's Functions and Dyson's Equation . . . . .	6
2.3	Dyson's Equation for One Scatterer . . . . .	7
2.4	Introducing a Second Scatterer . . . . .	7
2.5	Generalising to $N$ Scatterers . . . . .	8
<b>3</b>	<b>Results and Discussion</b>	<b>9</b>
3.1	Zero Scatterers (Pristine Equation) . . . . .	9
3.2	One Scatterer . . . . .	9
3.3	Two Scatterers . . . . .	10
3.4	$N$ Scatterers . . . . .	11
<b>4</b>	<b>Conclusions</b>	<b>12</b>
4.1	Conclusions from this Study . . . . .	12
4.2	Further Research . . . . .	13
<b>5</b>	<b>Acknowledgements</b>	<b>13</b>



# 1 Introduction

The aims of this project were to try to understand the physics of vibrations using a one dimensional model and to investigate how doping of a material would affect its acoustic properties. The ultimate goal is to solve the inverse problem, i.e. to determine how the mass of a material should be spatially distributed in order to generate a specific wave response.

## 1.1 Motivation

The motivation for the project comes from acoustic engineering and the construction of musical instruments.

The normal modes of vibration of a material are generally dependent on how its mass is distributed. Certain types of wood, from the so-called “tonewood trees”, have the ideal density and weight to make them suitable for the construction of guitars, violins and other instruments. Unfortunately many of these woods are being harvested using unsustainable forestry practices, and are becoming increasingly scarce.

NanoMusic is a multi-disciplinary project, coordinated by Prof Mauro Ferreira (TCD), which aims to introduce nanoparticles into wood pores in order to alter the mass distribution. This modifies the normal modes of vibration of the wood, and consequently its acoustic properties. It is hoped that by using this method, the high quality responses of Stradivarius instruments can be reproduced using ordinary pieces of wood.

The advantages of this approach are manifold. First, with an ability to engineer the acoustic properties of woods to suit our desires, the demand for the rare tonewoods will be greatly reduced, leading to a decrease in their deforestation. Because so many of the tonewood trees are now endangered, a shift in demand from these rare woods towards more sustainable types of wood will have an extremely positive impact on the environment. Furthermore, the use of more readily available woods for the design of instruments will minimise production costs.

There are also several benefits for the instruments themselves. Currently guitar and violin makers have a limited degree of control over the woods they use, due to the inherent variability between separate pieces of wood (even those which are taken from the same log). With NanoMusic, they will be able to fine-tune the acoustic properties to suit their needs, damping out unwanted frequencies and amplifying the most desirable frequencies. It will also be possible to increase the structural stability of the instrument, reducing any adverse effects caused by changes in moisture levels and other atmospheric conditions.

NanoMusic is still in its early stages. In order to obtain funding for the proposal, sufficient evidence must be found to show that nanoparticle doping does in fact alter

the acoustic properties of a piece of wood. Current work is being done on both the experimental and theoretical sides in order to show that this is the case, and the results have been promising. This project focuses on the theoretical and computational aspects of the problem.

## 1.2 Simplifications and Assumptions

This project aims to study the underlying physics of the problem, and is essentially a qualitative study into the effects of nanoparticle doping on the acoustic properties of a material. Therefore several assumptions were made in order to reduce the problem to its simplest form. The results presented do not correspond to any real-life system, but merely serve to demonstrate whether or not the introduction of nanoparticles affects the acoustic response of a material.

In order to study the fundamental physics of the problem, a one-dimensional model was used. The wave equation was not modified to reflect the type of material used (i.e. wood). It was assumed that the material was completely homogeneous before insertion of nanoparticles and any boundary conditions were neglected. Thus the model consisted of vibrations propagating along an infinitely long homogeneous string. Nanoparticles were modelled as point particles (or delta functions) positioned at specific points along the string. Effects of mass variations other than short range scatterers were not considered.

# 2 Theory and Methods

## 2.1 The Wave Equation

The wave equation in one dimension is as follows:

$$\frac{\partial^2 \psi}{\partial x^2} - \frac{1}{v^2} \frac{\partial^2 \psi}{\partial t^2} = 0 \quad (1)$$

where  $v$  is the speed of the wave. Linearity of the wave equation means that we can consider oscillations in a single frequency  $\omega$ , since the general result may be found by summing up contributions from all frequencies. If we assume that the function can be written as  $\psi(x, t) = \psi(x)e^{i\omega t}$ , the above PDE can be rewritten as

$$\frac{d^2 \psi}{dx^2} + \frac{\omega^2}{v^2} \psi = 0 \quad (2)$$

This is the homogeneous wave equation (i.e. without any point particles or scatterers), and will be hereafter referred to as the “pristine” equation.

It is known [1] that the speed  $v$  of a transverse wave on a homogeneous string is given by  $v^2 = T/\mu$  (where  $T$  is the tension in the string and  $\mu$  is the linear mass density). Indeed for most types of mechanical wave we have  $v^2 \propto 1/\mu$ . We therefore postulate that this is true in general, i.e. that if we have a non-homogeneous string with mass distribution  $\mu(x)$  then the speed of a wave at any point can be given by  $v(x)^2 \propto 1/\mu(x)$ . Therefore any variation in mass can be represented as a variation in velocity in the wave equation.

## 2.2 Green's Functions and Dyson's Equation

Returning to the pristine equation from before (Equation (2)), we have

$$\frac{d^2\psi}{dx^2} + \frac{\omega^2}{v_0^2}\psi = 0 \quad (3)$$

where  $v_0$  is the homogeneous wave speed. We can associate with this differential equation a Green's function  $\hat{g}$ , which we will call the "pristine Green's function".

Now again consider the nonhomogeneous case, i.e. the case with non-constant  $v$ . Here we have

$$\frac{d^2\psi}{dx^2} + \frac{\omega^2}{v(x)^2}\psi = 0 \quad (4)$$

This equation can be rearranged to give

$$-\frac{d^2\psi}{dx^2} + \frac{\omega^2}{v_0^2} \left[ 1 - \left( \frac{v_0}{v(x)} \right)^2 \right] \psi = \frac{\omega^2}{v_0^2} \psi \quad (5)$$

In this form, parallels between this equation and the Schrödinger Equation of quantum mechanics can be clearly seen, where we have

$$E \equiv \frac{\omega^2}{v_0^2} \quad (6)$$

and

$$V(x) \equiv \frac{\omega^2}{v_0^2} \left[ 1 - \left( \frac{v_0}{v(x)} \right)^2 \right] \quad (7)$$

We can associate with Equation (5) a second Green's function,  $\hat{G}$ .

Having reduced the problem to that of solving the Schrödinger Equation for a given potential  $V(x)$ , well-known results from quantum mechanics may now be used in order to find a solution. One such result is Dyson's Equation [2], which states that for a

perturbation  $\hat{H} = \hat{H}_0 + \hat{V}$  of the Hamiltonian, we have

$$\hat{G} = \hat{g} + \hat{g}\hat{V}\hat{G} \quad (8)$$

where  $\hat{g}$  is the pristine Green's function associated with the unperturbed Hamiltonian  $\hat{H}_0$ , and  $\hat{G}$  is the Green's function associated with the perturbed Hamiltonian  $\hat{H}$ .

The Green's function  $\hat{G}(x, x')$  corresponds to the acoustic reponse to an excitation at  $x'$  measured at  $x$ . Thus if the Green's function corresponding to a particular differential operator is known, then the response of the system to any excitation can be found by integrating the Green's function over the total excitation.

### 2.3 Dyson's Equation for One Scatterer

To simplify calculations, set  $v_0 = 1$ . The Green's function  $\hat{g}$  for the pristine equation can be found analytically using contour integration [3] and is given in Fourier space by

$$g(x, x', \omega) = -\frac{i}{2\omega} e^{i\omega|x-x'|} \quad (9)$$

The potential  $V(x) = -\omega^2\lambda\delta(x - x_0)$  corresponds to a single scatterer of weight  $\lambda$  at  $x = x_0$ . This gives (in Fourier space)

$$G(x, x', \omega) = \frac{1}{2i\omega} e^{i\omega|x-x'|} + \frac{\lambda}{4} \frac{e^{i\omega(|x-x_0|+|x_0-x'|)}}{1 - \lambda\omega/2i} \quad (10)$$

This function can then be plotted using Mathematica for various positions of the source  $x'$ , detector  $x$  and scatterer  $x_0$ .

### 2.4 Introducing a Second Scatterer

Adding a second scatterer makes the equations somewhat more complicated, and it is easier to perform the analysis using matrices. Suppose we have two localised impurities of weights  $\lambda_1$  and  $\lambda_2$  positioned at points  $x_1$  and  $x_2$  respectively. This corresponds to a potential

$$V(x) = -\omega^2\lambda_1\delta(x - x_1) - \omega^2\lambda_2\delta(x - x_2) \quad (11)$$

Using Dyson's Equation, we have

$$\begin{aligned} G(x, x') &= g(x, x') + \int_{-\infty}^{+\infty} dx'' g(x, x'')V(x'')G(x'', x') \\ &= g(x, x') - \omega^2g(x, x_1)\lambda_1G(x_1, x') - \omega^2g(x, x_2)\lambda_2G(x_2, x') \end{aligned} \quad (12)$$

Now we can find  $G(x_1, x')$  and  $G(x_2, x')$  by setting  $x = x_1$  and  $x = x_2$  in Equation (12), creating the following system of equations:

$$\begin{aligned} \begin{pmatrix} G(x_1, x') \\ G(x_2, x') \end{pmatrix} &= \begin{pmatrix} g(x_1, x') \\ g(x_2, x') \end{pmatrix} + \begin{pmatrix} -\omega^2 g(x_1, x_1)\lambda_1 & -\omega^2 g(x_1, x_2)\lambda_2 \\ -\omega^2 g(x_2, x_1)\lambda_1 & -\omega^2 g(x_2, x_2)\lambda_2 \end{pmatrix} \begin{pmatrix} G(x_1, x') \\ G(x_2, x') \end{pmatrix} \\ \Rightarrow \begin{pmatrix} G(x_1, x') \\ G(x_2, x') \end{pmatrix} &= \left[ I - \begin{pmatrix} -\omega^2 g(x_1, x_1)\lambda_1 & -\omega^2 g(x_1, x_2)\lambda_2 \\ -\omega^2 g(x_2, x_1)\lambda_1 & -\omega^2 g(x_2, x_2)\lambda_2 \end{pmatrix} \right]^{-1} \begin{pmatrix} g(x_1, x') \\ g(x_2, x') \end{pmatrix} \end{aligned} \quad (13)$$

Substituting this result back into the original expression gives

$$\begin{aligned} G(x, x') &= g(x, x') + \begin{pmatrix} g(x, x_1) & g(x, x_2) \end{pmatrix} \begin{pmatrix} -\omega^2 \lambda_1 & 0 \\ 0 & -\omega^2 \lambda_2 \end{pmatrix} \\ &\times \left[ I - \begin{pmatrix} g(x_1, x_1) & g(x_1, x_2) \\ g(x_2, x_1) & g(x_2, x_2) \end{pmatrix} \begin{pmatrix} -\omega^2 \lambda_1 & 0 \\ 0 & -\omega^2 \lambda_2 \end{pmatrix} \right]^{-1} \begin{pmatrix} g(x_1, x') \\ g(x_2, x') \end{pmatrix} \end{aligned} \quad (14)$$

This function can again be plotted using Mathematica for various positions of the source  $x'$ , detector  $x$  and scatterers  $x_1$  and  $x_2$ . In this project, the results were compared with those obtained by simply superimposing the results for two single scatterers, in order to examine the importance of the back scattering terms.

## 2.5 Generalising to $N$ Scatterers

The above matrix equation can be generalised quite easily to an arbitrary number of scatterers:

$$\begin{aligned} G(x, x') &= g(x, x') + \begin{pmatrix} g(x, x_1) & \cdots & g(x, x_N) \end{pmatrix} \begin{pmatrix} -\omega^2 \lambda_1 & \cdots & 0 \\ \vdots & \ddots & \vdots \\ 0 & \cdots & -\omega^2 \lambda_N \end{pmatrix} \\ &\times \left[ I - \begin{pmatrix} g(x_1, x_1) & \cdots & g(x_1, x_N) \\ \vdots & \ddots & \vdots \\ g(x_N, x_1) & \cdots & g(x_N, x_N) \end{pmatrix} \begin{pmatrix} -\omega^2 \lambda_1 & \cdots & 0 \\ \vdots & \ddots & \vdots \\ 0 & \cdots & -\omega^2 \lambda_N \end{pmatrix} \right]^{-1} \begin{pmatrix} g(x_1, x') \\ \vdots \\ g(x_N, x') \end{pmatrix} \end{aligned} \quad (15)$$

In this way it is possible to introduce any distribution of scatterers, each one defined by its position  $x_i$  and weight  $\lambda_i$ . By taking the limit  $N \rightarrow \infty$ , one can arrange the scatterers to form an arbitrary mass distribution.



### 3 Results and Discussion

#### 3.1 Zero Scatterers (Pristine Equation)

The equation was first solved in the pristine case, i.e. with no scatterers present. In Figure 1, the results are plotted both in Fourier space and in real space for a source at  $x' = 0$  and detector at  $x = 12$ .<sup>1</sup> It is clear from Figure 1b that the signal takes 12 units of time to arrive at the detector. This time delay is due to the finite speed of the signal (as mentioned previously,  $v$  was set equal to one for convenience). Once the signal has reached the detector, the response remains constant at  $-1/2$ .

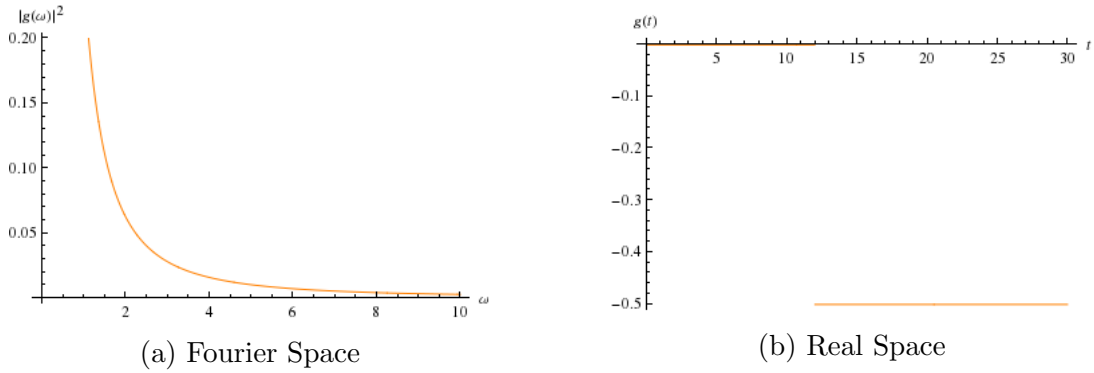


Figure 1: Pristine Green's function plotted in (a) Fourier space and (b) real space.

#### 3.2 One Scatterer

The Green's function for a single point scatterer was plotted for various positions of the scatterer. As an example, the results for a scatterer at  $x_0 = 4$  and for a scatterer at

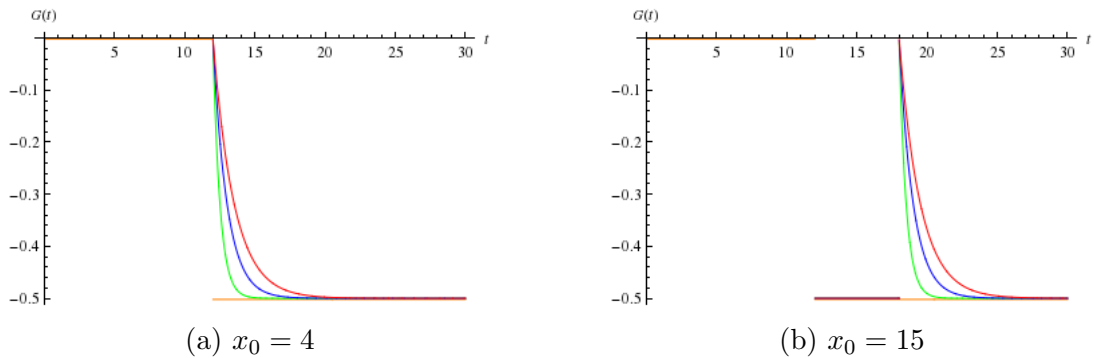


Figure 2: Green's functions for a single scatterer of various weights ( $\lambda$ ). Orange: pristine; Green:  $\lambda = 1$ ; Blue:  $\lambda = 2$ ; Red:  $\lambda = 3$

<sup>1</sup>The positions of source and detector were kept constant at  $x' = 0$  (source) and  $x = 12$  (detector) for all calculations performed in this project.

$x_0 = 15$  are shown in Figure 2.

In the first case, the scatterer is positioned between the source and the detector, and the resulting Green's functions are shown in Figure 2a for various values of  $\lambda$  (the weight of the delta function). As in the pristine case, it takes 12 units of time for the signal to arrive; however, the signal becomes less sharp and more gradual as  $\lambda$  increases.

In Figure 2b, the scatterer is positioned beyond the detector. Here the signal arrives in two distinct parts, the first being the direct signal (taking 12 units of time to arrive, as expected) and the second being the scattered signal, which arrives after 18 units of time - corresponding exactly with the time needed to travel from the source to the scatterer and then straight back to the detector. Note that the scattered signal is much less sharp than the direct signal, and its sharpness decreases with increasing  $\lambda$ .

### 3.3 Two Scatterers

When more than one scatterer was introduced, transforming back from Fourier space to real space became more difficult, and it was decided that it was not worth the computational time and efforts required. Instead, the remainder of the calculations in the project were performed in Fourier space. For comparison with the pristine solution in Fourier space, refer back to Figure 1a.

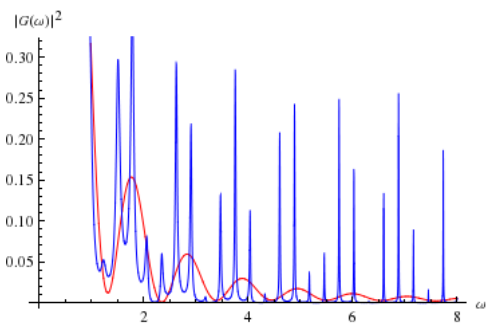


Figure 3: Comparison of matrix method (blue) with single scatterer first approximation method (red) for two scatterers positioned at  $x_1 = 4$  and  $x_2 = 15$ .

In the case of more than one scatterer, matrix methods were required to solve the problem (as shown in Section 2.5). The explanation for this is as follows. When there is only one scatterer present, only one scattering event takes place, and it occurs at the moment that the signal reaches the position of the scatterer. However, when a second scatterer is also included, one must take into account the possibility of back-scattering between the two scatterers. In principle, this could go on indefinitely, leading to an infinite number of scattering events. It is possible that the first scattering event may be so large in comparison to subsequent

events that the latter can be deemed negligible; if this is the case then the methods of the previous section can be employed as a first approximation to the solution, which only takes into account the first scattering event. To investigate whether or not this is possible, both methods were used to find the Green's function for two scatterers located at  $x_1 = 4$  and  $x_2 = 15$ . The results are shown in Figure 3. It is clear from the plot that back-scattering does have a significant effect on the result, and cannot be neglected when

dealing with multiple scatterers. The full matrix method was therefore employed for the remainder of the calculations.

The effect of varying the weight  $\lambda_i$  of one of the two scatterers was then investigated, and the results are shown in Figure 4. In the case where the point of greater weight was positioned between the source and detector, the effect was to decrease the magnitude of the Green's function (Figure 4a). In contrast, when the point of greater weight was positioned outside the region between the source and detector, the effect was to *increase* the magnitude of the Green's function (Figure 4b). These calculations were repeated for other positions of the scatterers, and this trend was found to be true generally. A possible explanation is that a larger scatterer in general leads to a larger amount of back-scattering. Therefore if the scatterer positioned beyond the detector has the greater weight, it will tend to deflect the signal back towards the detector, while if its weight is relatively smaller it will transmit more of the signal away from the detector.

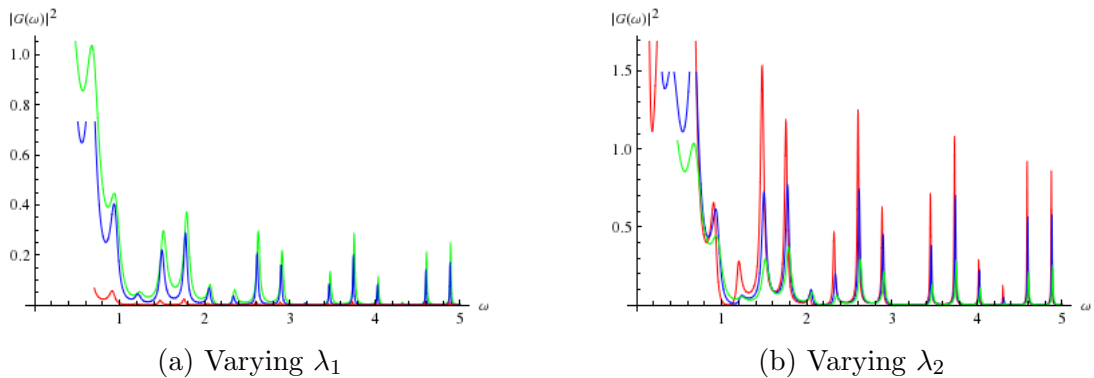


Figure 4: Varying the weights (a)  $\lambda_1$  and (b)  $\lambda_2$  for scatterers at  $x_1 = 4$  and  $x_2 = 15$ . Green:  $\lambda_i = 1$ ; Blue:  $\lambda_i = 2$ ; Red:  $\lambda_i = 10$

### 3.4 $N$ Scatterers

As discussed in Section 2.6, the matrix method can be extended to include an arbitrary number of scatterers. It was found that for larger values of  $N$  and evenly spaced scatterers, only very specific values of  $\omega$  were amplified. As before, varying the values of  $\lambda_i$  merely changed the strength of the resulting signal. As an example, the case  $N = 10$  was taken, and the resulting Green's functions were plotted for various distributions of the scatterers (see Figure 5).<sup>2</sup>

It is clear from the figures that the system allows only certain specific frequencies to be amplified, while the remaining frequencies are suppressed. If we ignore the first peak, which is most likely due to the non-scattered component of the signal, the remaining

<sup>2</sup>In all cases the weights were kept constant at  $\lambda_i = 10 \forall i$ .

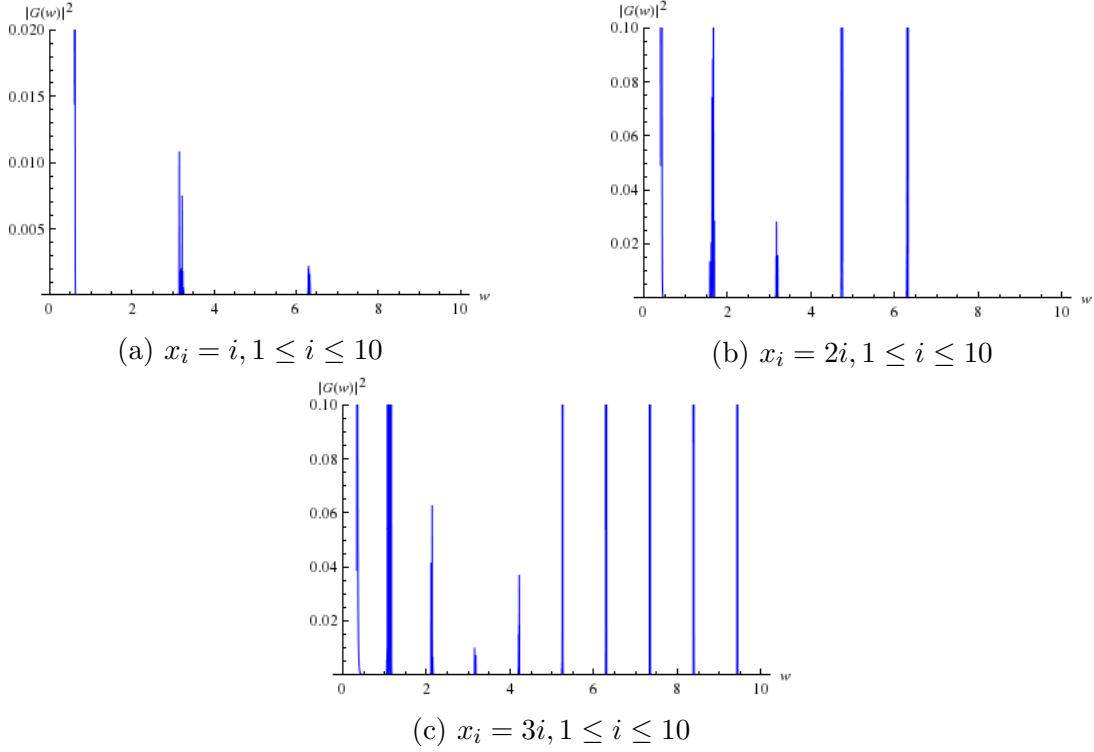


Figure 5: Green’s functions for various distributions of 10 equally weighted scatterers.

peaks appear to be multiples of the lowest frequency peak, which we could term the “fundamental frequency”. It is also interesting to note that when the spacing between scatterers is doubled or tripled (as is the case in Figures 5b and 5c respectively), the fundamental frequencies are one half and one third of the original value respectively. This is very like the behaviour seen in a string fixed at both ends, and suggests that the peaks may occur at these values as a result of standing waves developing between the scattering points.

## 4 Conclusions

### 4.1 Conclusions from this Study

The primary aim of this project was to try to understand how doping of a material affects its acoustic properties, using a highly simplified and idealised model. In the pristine case, a point source led to a sharp response as soon as the signal reached the detector. When a single scatterer was introduced the result was similar, except that the arrival of the signal at the detector was more gradual. However, once multiple scatterers were introduced, it was found that the system allowed only certain specific frequencies to be transmitted to the detector. In the case where the scatterers were evenly spaced, the frequencies

transmitted appeared to be multiples of a “fundamental frequency”, analogous to the fundamental frequencies observed in a string fixed at both ends. Varying the weights of the scatterers affected only the strength of the signal, and not the frequencies transmitted.

The results of this project are very encouraging as a first step towards solving the inverse problem, i.e. determining the positions and masses of scatterers required to generate a specific wave response. Suppose one has a target response, such as that of a Stradivarius instrument to a point disturbance. This ideal response can be written in terms of its Fourier components, giving an ideal distribution of frequencies. In this project, an exact quantitative relationship between the positions of the scatterers and the resulting frequency distribution was not found. However, it can be seen qualitatively from Figure 5 that the positions of the scatterers have a clear and direct effect on the frequency response produced. Thus it is conceivable that, in principle, any given frequency distribution could be constructed by varying the positions of scatterers in the material.

## 4.2 Further Research

The next step is to carry out a quantitative study of the system, and to find the exact relationship between the positions of the scatterers and the response generated. When such a relationship has been found, it will be possible to focus on the inverse problem. One possible approach to this would be to use a variational method. A functional could be defined with the mass distribution function as an input and the deviation from the ideal solution as an output. Then to solve the problem one would have to search for a distribution function that would minimise the value of the functional.

Other further developments to this project would include relaxing some of the simplifying assumptions made in the beginning. For example, one could introduce boundary conditions, or extend the model to two or three dimensions. By making the system less idealised and more like a real life situation, the results will become more intuitive and relevant to the overall problem. Furthermore, when the major idealisations have been removed, the theories presented here will become testable by experiment. This would provide a chance both to confirm the results given by the theory and to find out what other factors must be taken into account.

## 5 Acknowledgements

I would like to thank my project partner Mauresse Gargan for all her hard work throughout the past few months, and our supervisor Prof Mauro Ferreira for his invaluable guidance and support.

## References

- [1] Young, H. D. & Freedman, R. A. (2008), *University Physics*, Pearson Education, Inc., San Francisco
- [2] Economou, E.N. (1979), *Green's Functions in Quantum Physics*, Springer, Berlin
- [3] Priestley, H.A. (1985), *Introduction to Complex Analysis*, Oxford University Press Inc., New York

